Cross-stacked carbon nanotube film as an additional built-in current collector and adsorption layer for high-performance lithium sulfur batteries

2016 Nanotechnology 27 075401

(http://iopscience.iop.org/0957-4484/27/7/075401)

IOP Publishing Nanotechnology
Nanotechnology 27 (2016) 075401 (9pp) doi:10.1088/0957-4484/27/7/075401

Cross-stacked carbon nanotube film as an additional built-in current collector and adsorption layer for high-performance lithium sulfur batteries

Li Sun[1,2], Weibang Kong[2], Mengya Li[2], Hengcai Wu[2], Kaili Jiang[2,3], Qunqing Li[2,3], Yihe Zhang[1], Jiaping Wang[2,3] and Shoushan Fan[2]

[1] Beijing Key Laboratory of Materials Utilization of Nonmetallic Minerals and Solid Wastes, National Laboratory of Mineral Materials, School of Materials Science and Technology, China University of Geosciences, 100083 Beijing, People's Republic of China
[2] Department of Physics and Tsinghua-Foxconn Nanotechnology Research Center, Tsinghua University, Beijing 100084, People's Republic of China
[3] Collaborative Innovation Center of Quantum Matter, Beijing 100084, People's Republic of China

E-mail: sunli@cugb.edu.cn and jpwang@tsinghua.edu.cn

Received 27 October 2015, revised 21 November 2015
Accepted for publication 7 December 2015
Published 18 January 2016

Abstract

Cross-stacked carbon nanotube (CNT) film is proposed as an additional built-in current collector and adsorption layer in sulfur cathodes for advanced lithium sulfur (Li-S) batteries. On one hand, the CNT film with high conductivity, microstructural rough surface, high flexibility and mechanical durability retains stable and direct electronic contact with the sulfur cathode materials, therefore decreasing internal resistivity and suppressing polarization of the cathode. On the other hand, the highly porous structure and the high surface area of the CNT film provide abundant adsorption points to support and confine sulfur cathode materials, alleviate their aggregation and promote high sulfur utilization. Moreover, the lightweight and compact structure of the CNT film adds no extra weight or volume to the sulfur cathode, benefitting the improvement of energy densities. Based on these characteristics, the sulfur cathode with a 100-layer cross-stacked CNT film presents excellent rate performances with capacities of 986, 922 and 874 mAh g^{-1} at cycling rates of 0.2C, 0.5C and 1C for sulfur loading of 60 wt%, corresponding to an improvement of 52%, 109% and 146% compared to that without a CNT film. Promising cycling performances are also demonstrated, offering great potential for scaled-up production of sulfur cathodes for Li-S batteries.

Keywords: Li-S battery, CNT film, current collector, adsorption layer

(Some figures may appear in colour only in the online journal)

1. Introduction

Lithium sulfur (Li-S) batteries are regarded as one of the most attractive candidates for next-generation rechargeable battery systems due to their high theoretical energy density, low cost and environmental friendliness [1–3]. Practical application of the Li-S battery is generally hindered by some noticeable problems. Firstly, the poor ionic and electronic conductivities of sulfur and its various discharge products (Li_2S_x, $x = 1 \sim 8$) result in large polarization and poor active material utilization, limiting the practical capacities of the cathode [4]. Secondly, the dissolution of polysulfide intermediates in electrolyte and the so-called 'shuttle effect' give rise to rapid capacity fade during extended cycling, leading to poor cycling reversibility [5]. Thirdly, the volume variation of sulfur upon Li uptake makes Li_2S pulverize and lose its electrical contact with the

conductive substrate or the current collector, giving rise to mechanical failure of the electrode structure [4]. These problems cause small capacity, large capacity fade and poor mechanical performances of sulfur cathodes, making pure sulfur unsuitable for direct use as a cathode material [6].

One approach to improve the electrochemical performance of sulfur cathodes is to combine sulfur with conductive carbon materials, represented by carbon nanotubes (CNTs) [7–9], graphene [10, 11] and porous carbon materials [12, 13]. The structures of the carbon materials have been carefully designed with several aspects including: (1) high conductivity to provide continuous electronic contact, (2) well-preserved confined structures (cavities, pores or channels, etc) to restrain sulfur on the cathode side, and (3) high flexibility to accommodate the volume variation of sulfur and buffer the stress during cycling. Of all the carbon materials to host sulfur, CNTs were demonstrated to be among the most promising. With some unique properties including large surface area, low weight, high electrical conductivity and superior mechanical flexibility, CNTs can efficiently trap elemental sulfur within their matrix and achieve impressive electrochemical performances [9]. Various Li-S/CNT batteries have been proposed with excellent capacities and high reversibility [7–9]. However, some of the carbon materials with confined structures, such as the tortuous interior pores or the core–shell architecture, hinder effective electrolyte soakage, impede rapid lithium ion transport, and therefore limit the high-rate electrochemical performances.

Recently, employing an interlayer between the sulfur cathode materials and separator has shown large potential in improving the electrochemical performance of Li-S batteries. Flexible and highly conductive carbonaceous interlayers, including CNTs [14], microporous carbon [15], graphene [11, 16, 17] and Al_2O_3-deposited carbon cloth [18], have been developed as physical or chemical barriers to impede the shuttle of polysulfides and have demonstrated enhanced cycling stability. Similarly to the carbonaceous confined materials, synthesis of these carbonaceous interlayers also involved complex procedures (atomic layer deposition [18], filtration [14], etc) or introduction of inert components (binder [15], carbon black [16], etc), which added substantial cost and additional weight/volume to the battery. To compromise the inert components and simplify the preparation procedures, very thin graphene membranes were coated onto a routine polymer separator [11, 17] to block the diffusion of polysulfides. High homogeneity remained a problem in the coating process.

Here, cross-stacked CNT film was employed as an additional built-in current collector and adsorption layer in Li-S batteries. The CNT film was prepared by cross-stacking several layers of super-aligned CNT (SACNT) layers. With attractive features in conductivity, mechanical strength, flexibility and porosity, the cross-stacked CNT film has several functions, including: 1) retaining stable and direct electronic contact with the sulfur slurry for electron transfer, 2) providing abundant adhesion points to adsorb sulfur cathode materials, 3) ensuring easy electrolyte infiltration, and 4) accommodating the volume variation and benefitting rapid ion transportation. Therefore, polarization of the cathode and loss of sulfur are successfully impeded, giving rise to high sulfur utilization, improved cycling stability and excellent rate capability. Moreover, the cross-stacked CNT film was lightweight with low thickness, thus avoiding the additional introduction of inert components to the cathode and benefitting the improvement of energy densities. In addition, the incorporation of the cross-stacked CNT film allows the preparation of sulfur cathodes via the traditional slurry-coating method using the commercial pure sulfur powder, which significantly lowers the cost, simplifies the synthesis procedure and provides great potential for scaled-up manufacturing of Li-S batteries.

2. Experimental section

2.1. Fabrication of CNT films

SACNT arrays with a tube diameter of 20 ∼ 30 nm and a height of 300 μm were synthesized on silicon wafers by chemical vapor deposition, with iron as the catalyst and acetylene as the precursor. Details of the synthesis procedure can be found in previous papers [19–21]. Continuous SACNT films can be directly drawn from SACNT arrays by an end-to-end joining mechanism [19, 20, 22]. CNT films (10 cm × 10 cm) were prepared with 50 and 100 cross-stacked CNT layers. After soaking with ethanol and drying, the CNT films were laser cut into square pieces for use, each with a width of 13 mm.

2.2. Characterization and electrochemical measurement

The microstructure and elemental analysis of the CNT film were characterized by scanning electron microscopy (SEM, Sirion 200, FEI) and transmission electron microscopy (TEM, Tecnai G2F20, FEI).

The sulfur slurry was prepared by thoroughly mixing a N-methyl-2-pyrrolidine solution with sulfur powder (Beijing Dk Nano Technology Co., Ltd), conductive Super P, and poly (vinyl difluoride) binder at a weight ratio of 5:4:1 and 6:3:1. Afterward, the slurry was deposited on an aluminum foil (21.5 μm in thickness) followed by drying in a vacuum oven at 50 °C overnight to obtain the sulfur cathode.

Coin-type half-cells were assembled in a glove box filled with protective argon gas (M Braun Inert Gas Systems Co. Ltd, Germany) with the slurry-coated sulfur cathode (diameter, 10 mm) as the working electrode and pure lithium foil as the reference electrode. The square CNT film with 50 or 100 layers of cross-stacked CNT film was placed onto the sulfur cathode. The width of the CNT film was slightly larger than the diameter of the sulfur cathode to ensure efficient surface coverage. A polypropylene film (Celgard 2400) was used to separate the cathode and the anode. A 1 mol l^{-1} lithium bis (trifluoromethanesulfonyl) imide (LiTFSI) and 0.2 mol l^{-1} $LiNO_3$ in dimethyl ether and 1, 3-dioxolane (DOL) with a volume ratio of 1:1 was used as the electrolyte. The cycling tests were made on a Land battery test system

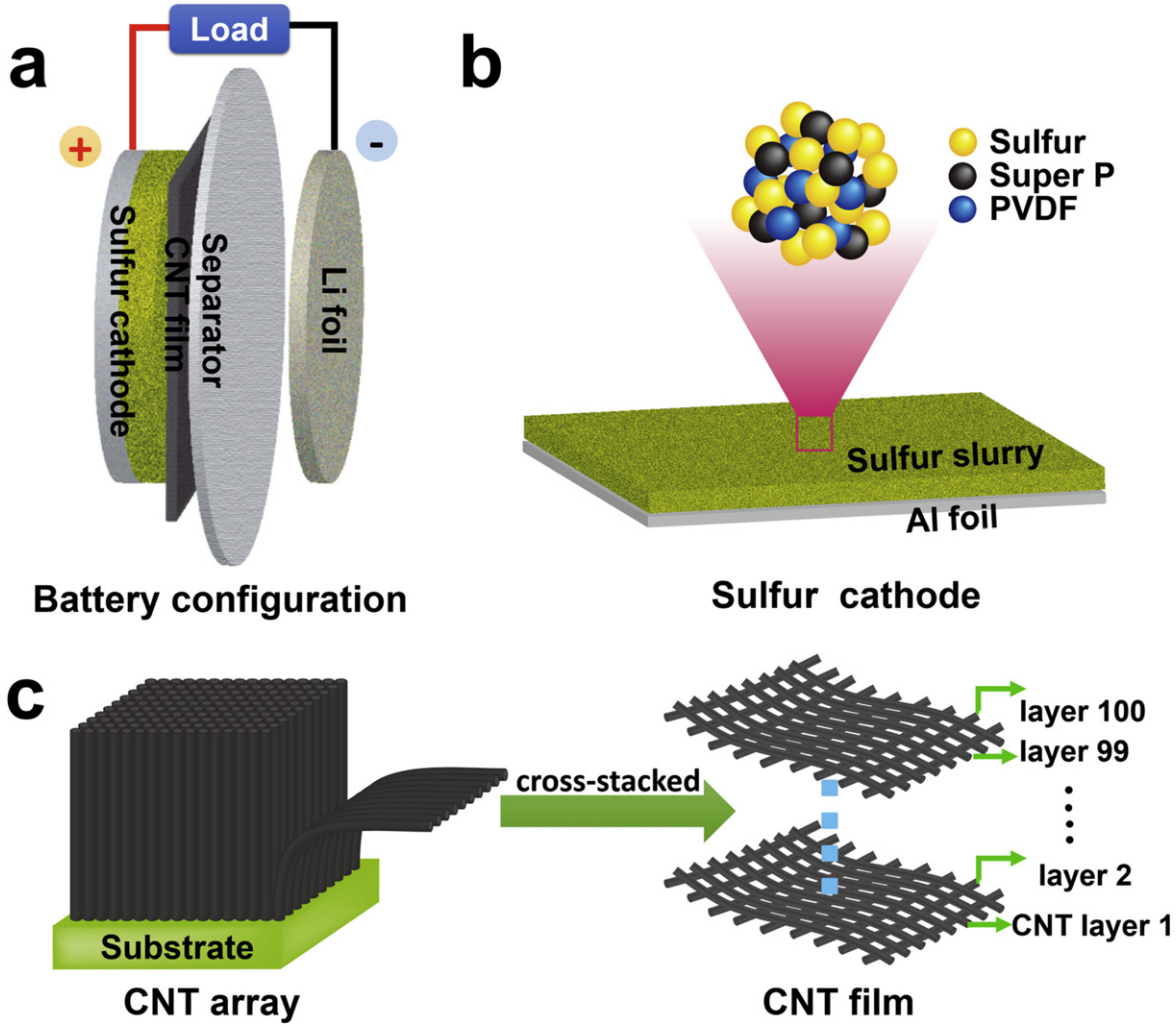

Figure 1. Schematic of the (a) battery configuration, (b) cathode structures, (c) CNT array and cross-stacked CNT film.

(Wuhan Land Electronic Co., China) in 1.8 ~ 2.6 V at different charge/discharge rates. The rate tests were performed by charging the electrode at varied charge rates while discharging at a constant rate of 0.2C. The electrochemical impedance spectroscopy (EIS) and cyclic voltammetry (CV) measurement were performed on a potentiostat/galvanostat (EG&G Princeton Applied Research 273A).

3. Results and discussion

The configuration of the Li-S battery with a built-in CNT film is schematically illustrated in figure 1(a). The cathode slurry was prepared by dispersing commercial sulfur, conductive super P and poly(vinyl difluoride) (5:4:1 or 6:3:1 in weight) in N-methyl-2-pyrrolidine solution. Then the slurry was coated onto the Al foil via the commercially used slurry-coating method (figure 1(b)). The square CNT film was placed onto the well-cut circular sulfur cathode with full surface coverage. The detailed illustration in figure 1(c) shows the structure of the CNT array and the CNT film. The cross-stacked CNT layers in the CNT film offered continuous electron pathways and abundant adsorption points for the sulfur cathode materials. Note that the cross-stacked CNT film possesses a low weight and compressed structure. The average weight and overall thickness of the 100-layer film used in the battery was as small as 0.34 mg and 2.0 μm, respectively, which only accounts for 16.1% of the weight and 3.0% of the thickness of the sulfur slurries. For the 50-layer film, the values are even smaller, i.e. 8.0% of the weight and 1.8% of the thickness. The lightweight and ultrathin features of the CNT film avoid the introduction of extra weight and volume, therefore having little effect on the overall energy density of the cell. Figure 2(a) shows a photograph of the slurry-coated sulfur cathode and the cross-stacked CNT film. The CNT film can be easily buckled with tweezers without damage (figure 2(b)), which demonstrates excellent flexibility and high mechanical stability, favorable for long-term charge–discharge processes. The TEM image in figure 2(c) displays the morphology of one CNT. The visible graphitic layers offer excellent charge-transfer paths. The SEM images of the surface (figure 2(d)) and cross-section (figure 2(e)) of the CNT film reveal a regular cross-stacked configuration of the CNT film, in which the rough microstructural surface, highly porous microstructure

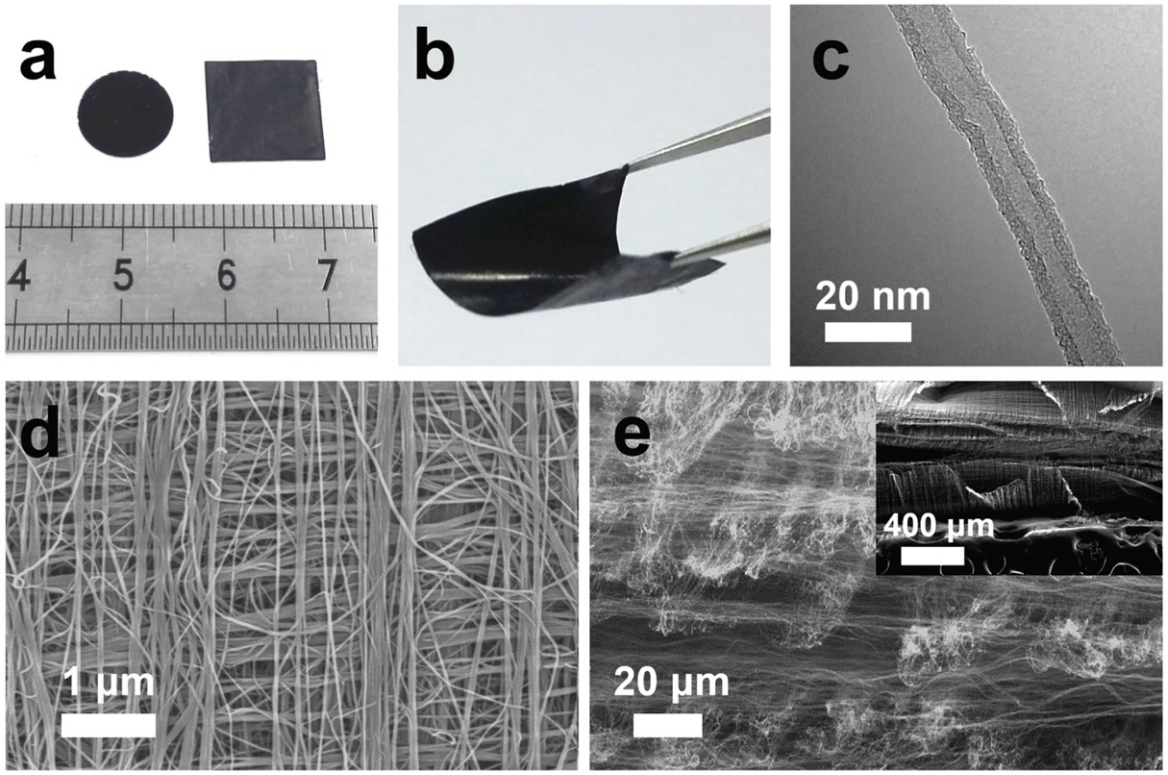

Figure 2. Photographs of (a) cathode film and corresponding CNT film. (b) CNT film showing good flexibility. (c) TEM image of the super-aligned CNT. SEM images of (d) surface and (e) cross-sectional morphology of the cross-stacked CNT film. The inset of (e) shows an image of the cross-section morphology at low magnification.

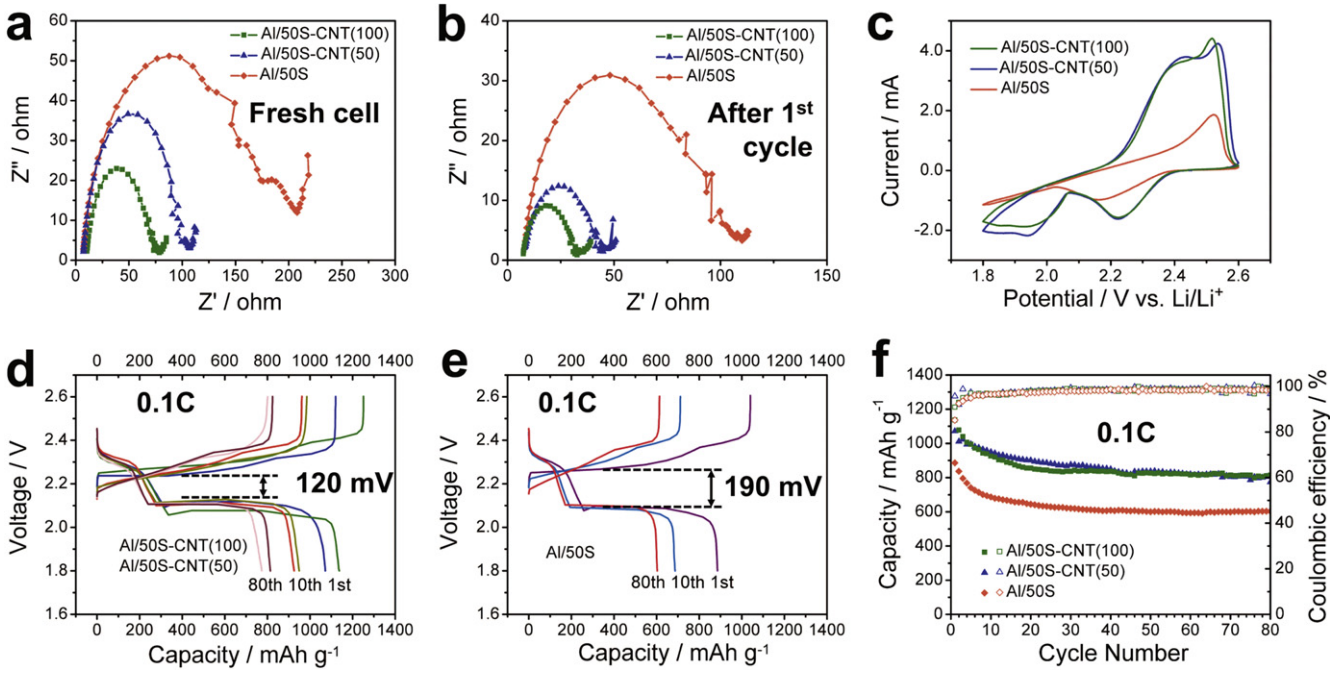

Figure 3. Electrochemical performances of the Li-S cells with Al/50S-CNT (100), Al/50S-CNT (50) and Al/50S cathodes. Electrochemical impedance spectroscopy plots of (a) the fresh cell and (b) the cell after the first cycle. (c) Cyclic voltammogram scans. Galvanostatic charge–discharge profiles of the Li-S cells (d) with Al/50S-CNT (100), Al/50S-CNT (50) and (e) the Al/50S cathodes. (f) Cycling performances at 0.1C.

and large surface area ensure effective electronic contact, sufficient electrolyte infiltration and fast redox reactions.

The influence of the CNT film on the electrochemical characteristics of the Li-S cell was examined by the EIS, which is one of the most powerful electroanalytical tools to study kinetics in various electrochemical systems [23–25]. The horizontal axis and the vertical axis correspond to the real (Z′) and imaginary part (Z″) of the complex impedance (Z), respectively. A typical EIS spectrum is normally composed of two depressed semicircles and an inclined line, of which the two semicircles are partially overlapped [23]. The diameter of the depressed semicircle in EIS spectra indicates the charge-transfer resistance [23]. As shown in figure 3(a), the cathodes with 100-layer and 50-layer CNT films, marked as Al/50S-CNT (100) and Al/50S-CNT (50), respectively, possessed a much lower resistance compared to that without a CNT film (Al/50S). This phenomenon was attributed to the multi-functional cross-stacked CNT film inserted in the cathodes. On one hand, the high conductivity of the CNT film made it an effective embedded current collector to serve as a supplement to Al foil, therefore promoting faster charge transfer and achieving significantly reduced internal resistance. On the other hand, the high flexibility and microstructural surface roughness of the CNT film ensured its close contact with the sulfur slurry, and therefore the contact resistance is effectively decreased, further contributing to the lower charge-transfer impedance. The EIS spectra after cycling demonstrated that all the cathodes presented decreased charge-transfer impedance (figure 3(b)) as a result of the initial wetting process between electrode and electrolyte. Similar to those before cycling, notably smaller charge-transfer impedances were also presented in Al/50S-CNT (100) and Al/50S-CNT (50). This was attributed to the effective adsorption of dissolved polysulfide intermediates in the CNT film and consequently inhibited formation of lithium sulfide layers on the metallic lithium during cycling. The EIS results also demonstrated that the introduction of the CNT film on the cathode did not hinder effective electrolyte infiltration and ion transport, which guaranteed high sulfur utilization and excellent rate performance.

The electrochemical kinetic process of the cathodes was further studied by the CV scans. As shown in figure 3(c), both the Al/50S-CNT (100) and Al/50S-CNT (50) cathodes exhibited two reduction peaks at the cathodic scans of around 2.2 and 2.0 V, presenting a typical two-step reduction of sulfur to high-order polysulfide and Li_2S/Li_2S_2, respectively. The oxidation peaks at around 2.4 and 2.5 V in the anodic scans corresponded to the transformation of Li_2S to high-order polysulfide and eventually to elemental sulfur. Suppressed polarization, high redox intensities and sharp peaks were observed in the cathodes with a CNT film, demonstrating favorable electrode dynamics. As a contrast, the CV profiles of the Al/50S cathode without a CNT film presented obviously broadened peaks and lower currents in both cathodic and anodic branches, indicating slower dynamics and high internal resistivity induced by the poor electronic contact between the sulfur and carbon black. In addition, the peaks corresponding to the transfer between the high-order polysulfide and Li_2S/L_2S_2 were almost unobservable in the Al/50S cathode, which also indicated the large polarization, sluggish kinetics, inferior liquid-to-solid conversion process and severe loss of polysulfides. These phenomena demonstrated that the unique cross-stacked CNT film was highly effective in improving the electrochemical behavior of the sulfur cathode by serving as an additional built-in current collector to retain high conductivity, as well as an adsorption layer to alleviate the loss of sulfur cathode materials and promote deep electrochemical reactions.

The cyclic performance of the sulfur cathodes was evaluated at a current density of 0.1C in the voltage window of 1.8 ∼ 2.6 V. Figures 3(d) and (e) show the respective discharge/charge voltage profiles of the cathodes with and without the CNT film, respectively. Consistent with those reported in the literature, typical two-plateau behavior was observed in all cathodes, corresponding to the formation of long-chain (high plateau at 2.3 V) and low-order polysulfides (low flat plateau at 2.0 V) during discharge [26–28]. Both cathodes with a CNT film, i.e., the Al/50S-CNT (100) and Al/50S-CNT (50) cathodes, exhibited long and flat plateaus stabilized at around 2.0 V, demonstrating the highly efficient lithiation of the intermediate polysulfides to final products of Li_2S/Li_2S_2. The low polarization of 120 mV implied by the voltage difference between charge and discharge plateaus reveals a kinetically efficient reaction process with a small barrier [11, 29]. In comparison, the cathode without a CNT film showed a much larger polarization of 190 mV and clear shift of the charge/discharge plateau during cycling, indicating slow redox reaction kinetics. Compared to Al/50S, both Al/50S-CNT (100) and Al/50S-CNT (50) delivered improved capacities (figure 3(f)), which was attributed to the well-embedded conductive network and continuous electron pathways offered by the CNT film. The largest capacities were achieved in Al/50S-CNT (100), and capacities of 1139, 953 and 815 mAh g^{-1} were exhibited in the first, second and 80th cycle, respectively; slightly larger than those of Al/50S-CNT (50). This might be attributed to the increased electronic conductive pathways and adsorption points in the 100-layer CNT film and consequently enhanced conductivity and protection to the sulfur cathode materials. In addition, capacity fade of 16.3% and 13.6% in the first ten cycles was found in the Al/50S-CNT (100) and Al/50S-CNT (50) cathodes, respectively, implying effective adsorption of the cathode materials by the CNT film. As a contrast, the Al/50S cathode showed significant capacity fade of 23.5% from 890 to 681 mAh g^{-1} in ten cycles, implying a severe loss of polysulfides.

In addition, the built-in CNT film also presented great efficiency in promoting high-rate capability. As shown in figure 4(a), the Al/50S cathode without a CNT film could only work at low cycling rates of 0.2 ∼ 1C, with inferior capacities of 861 ∼ 736 mAh g^{-1} at 0.2C, 725 ∼ 696 mAh g^{-1} at 0.5C and 622 ∼ 633 mAh g^{-1} at 1C. When higher current rates of 1.5 ∼ 3C were applied, the electrode failed with capacities declining to around zero. As a contrast, a greatly improved rate performance was delivered in cathodes with a CNT film. The largest capacities were obtained in

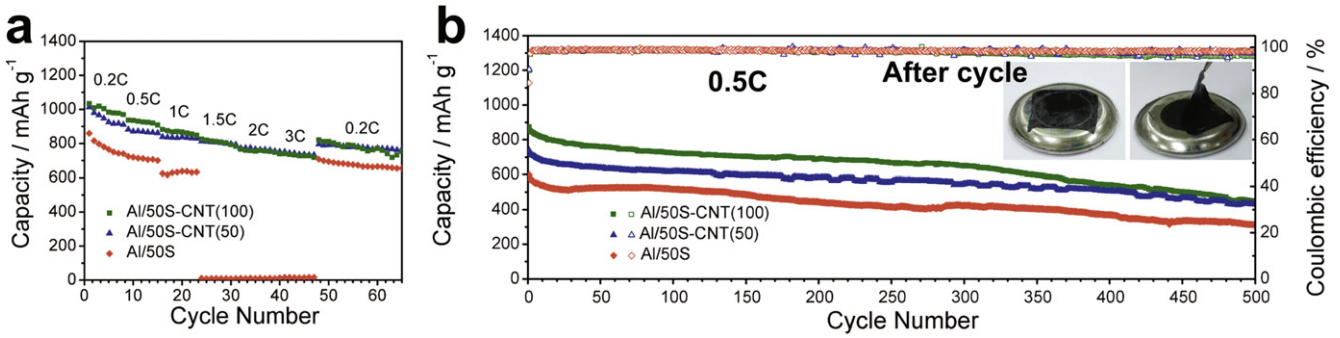

Figure 4. (a) Rate performances and (b) long-term cycling performances at 0.5C of the Li-S cells with Al/50S-CNT (100), Al/50S-CNT (50) and Al/50S cathodes. The inset of (b) shows photos of the CNT film after cycling.

Al/50S-CNT (100), with capacities of 1033 ~ 970 mAh g^{-1} at 0.2C, 938 ~ 905 mAh g^{-1} at 0.5C, 883 ~ 853 mAh g^{-1} at 1C, 832 ~ 788 mAh g^{-1} at 1.5C, 773 ~ 748 mAh g^{-1} at 2C and 748 ~ 729 mAh g^{-1} at 3C. After deep cycling at high rates, the capacities recovered to 828 mAh g^{-1} at 0.2C, implying a good reversibility. Compared to Al/50S-CNT (100), the Al/50S-CNT (50) exhibited smaller capacities at 0.2C ~ 1C due to the decreased electronic conductive pathways and adsorption points in the 50-layer CNT film. Meanwhile, a further increase of cycling rates to 1.5 ~ 3C brought comparable capacities in both batteries, possibly because the fast charge/discharge process allowed limited time for the loss of polysulfides and consequently weakened the effect of the film thickness. The larger capacities of the sulfur cathodes with CNT films were attested to the close electrical contact between sulfur active material and the CNT film that gave the cathode high conductivity for electron transport, the highly porous structure of the CNT film that allowed easy electrolyte penetration for efficient lithium ion transport, and the abundant adhesion points provided by the cross-stacked CNT multi-layers that alleviated loss of sulfur cathode materials and ensured high sulfur utilization. Long-term cycling behavior of the cathodes at 0.5C is demonstrated in figure 4(b). Superior initial capacities of 872 and 740 mAh g^{-1} were achieved in the Al/50S-CNT (100) and Al/50S-CNT (50) cathodes, larger than the 597 mAh g^{-1} in the Al/50S cathode, suggesting the advantage of the conductive CNT film in exerting high sulfur utilization and promoting deep lithiation. After 500 cycles, both Al/50S-CNT cathodes achieved stable performances with capacities around 460 mAh g^{-1}, also larger than the 307 mAh g^{-1} in the Al/50S cathode. Moreover, the cathode structure remained integral without visible alternation after cycling. As revealed by the photos shown in the inset of figure 4(b), the CNT film could still be easily detached from the cathode without damage and presented high flexibility, suggesting excellent mechanical stability. Both the excellent cycling stability and rate capability of the Al/50S-CNT cathodes reveal the advantage of the highly porous and conductive cross-stacked CNT film in facilitating electron and lithium ion diffusion and consequently achieving better sulfur utilization and higher specific capacity. In addition, the large surface area of the cross-stacked CNT film also alleviated the aggregation of sulfur cathode materials and the formation of the Li_2S blocking layer in the high-rate discharge process.

The microstructure of the CNT film after cycling was further analyzed by SEM, in which both 50-layer and 100-layer CNT films had similar morphologies, with no evident differences between the surface close to the separator and the one in contact with sulfur. A typical image of the microstructure without washing away the lithium salts (LiTFSI and $LiNO_3$) in the electrolyte is shown in figure 5(a), and the CNT film was covered by some large lithium salts. Meanwhile, after dissolving away these salts with DOL, the CNT film became highly porous, similar to that before cycling, with no large aggregates of sulfur or Li_2S/ Li_2S_2 (figure 5(b)). The energy-dispersive X-ray elemental analysis shown in the inset revealed the existence of elemental sulfur, indicating that sulfur particles were encapsulated into the porous film during the electrochemical process. This process is illustrated in figure 5(c). In the as-assembled cathode, sulfur particles were embedded in the slurry on the Al foil, and the CNT film placed onto it provided sufficient electron transfer paths. During the first discharge process, sulfur particles were lithiated to electrolyte-soluble polysulfides, some of which can easily spread into the CNT film. In the subsequent lithiation process, the high surface area of the CNT film provided abundant attachment points for nucleation and deposition of deep discharge products, creating well-embedded Li_2S/Li_2S_2 particles in the CNT network. The embedded Li_2S/Li_2S_2 particles can then be reversibly converted into sulfur and well distributed in the CNT network after the first charging of the cell. In the following discharge–charge cycles, the CNT film continued to provide both high conductivity and adsorption points to support the sulfur cathode materials, suppress their aggregation and alleviate their loss into the electrolyte.

To further investigate the efficiency of the CNT film as an additional built-in current collector and adsorption layer, cathodes with a higher sulfur loading of 60 wt% were also fabricated. As demonstrated in figures 6(a) and (b), when the CNT film was introduced, the cycling performances were greatly improved. Capacities of 930 ~ 641 and 843 ~ 568 mAh g^{-1} were obtained in 100 cycles at 0.1C for cathodes with 100-layer and 50-layer CNT films; i.e., Al/60S-CNT (100) and Al/60S-CNT (50), respectively,

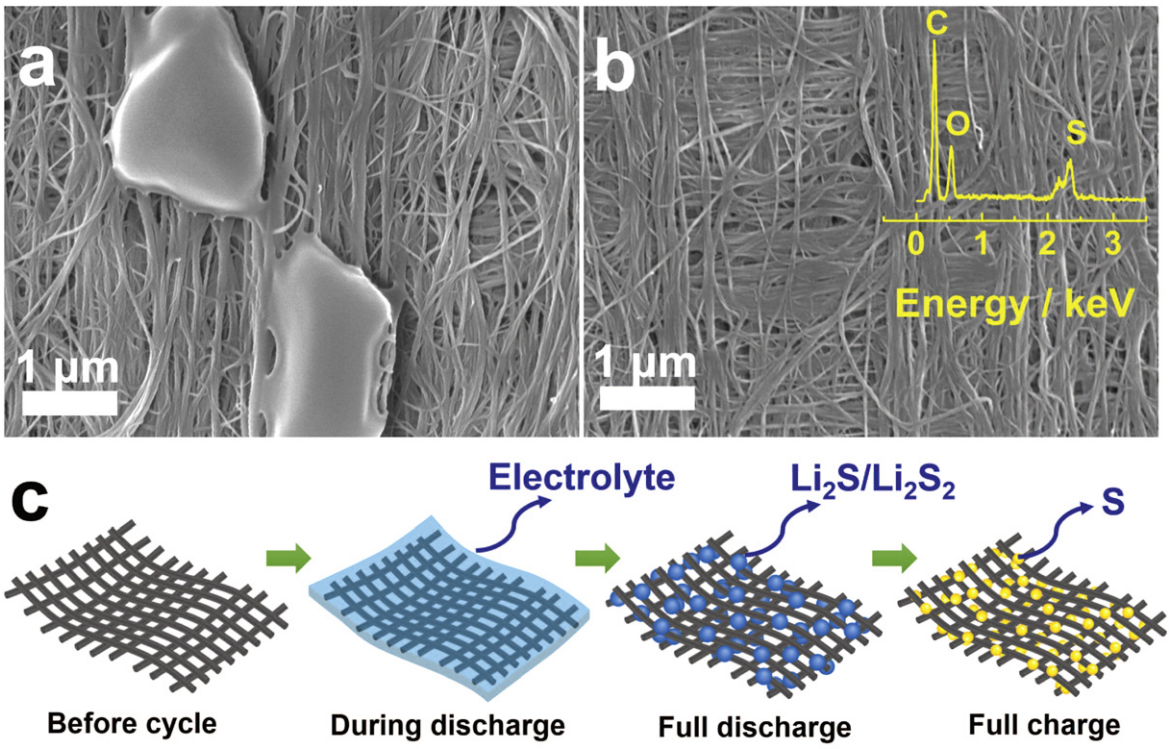

Figure 5. SEM images of the CNT film after cycling (a) without washing and (b) after washing. The inset of (b) shows the corresponding energy-dispersive x-ray elemental analysis. (c) Schematic of the structural variation of the CNT film during cycling.

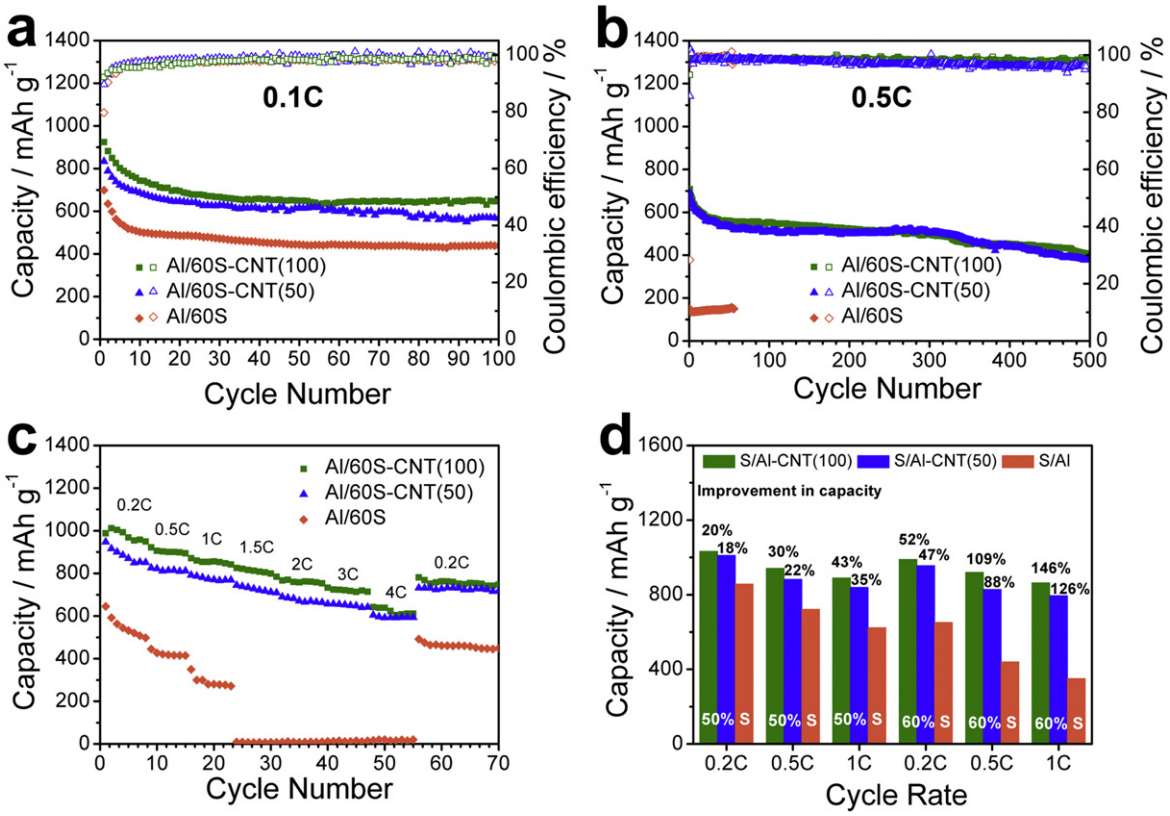

Figure 6. Electrochemical performances of the Li-S cells with Al/60S-CNT (100), Al/60S-CNT (50) and Al/60S cathodes. Cycling performances at (a) 0.1C and (b) 0.5C. (c) Rate performances. (d) Specific capacities at different rates for cathodes with 50 wt% and 60 wt% S.

corresponding to capacity decay of 0.31% and 0.32% per cycle. During the faster charge/discharge process at 0.5C, comparably stable cycling performances were delivered in both cathodes, with capacities of around 710 ~ 395 mAh g^{-1} and capacity decay of 0.089% per cycle in 500 cycles. In comparison, the capacity of the Al/60S cathode was 701 mAh g^{-1} at 0.1C, and this value collapsed to as little as 146 mAh g^{-1} at the elevated cycling rate of 0.5C. The function of the CNT film in promoting high-rate performances was also demonstrated. As presented in figure 6(c), excellent rate performance was achieved in the Al/60S-CNT (100) cathode with the highest discharge capacities of 986 ~ 949, 922 ~ 895, 874 ~ 847, 825 ~ 782, 767 ~ 751 and 740 ~ 718 mAh g^{-1} at 0.2C, 0.5C, 1C, 1.5C, 2C and 3C, respectively. Even at a high rate of 4C, it still achieved a high reversible capacity of 649 ~ 617 mAh g^{-1}. Moreover, after cycling at such a high rate, the capacity recovered to 783 mAh g^{-1} at 0.2C, implying good reversibility. The rate capability was much inferior for the Al/60S cathode, which could only work at small cycling rates of 0.2, 0.5 and 1C with lower capacities of 649 ~ 494, 445 ~ 413 and 349 ~ 274 mAh g^{-1}, respectively. When the cycling rates were raised to higher than 1.5C, the Al/60S cathode without a CNT film failed due to the inactive electrochemical process. It should be mentioned that the enhancement of sulfur loading is very difficult in Li-S batteries due to the small conductivity (5×10^{-30} S m^{-1}) of sulfur. Through employment of various carbonaceous materials to form carbon–sulfur composites, the reported sulfur loading can be generally raised to around 60 wt% with acceptable performances [30–32]. In this work, comparable sulfur loading and electrochemical performances were demonstrated simply by introducing a lightweight and ultrathin cross-stacked CNT film as an additional built-in current collector and adsorption layer, which allowed the use of pure sulfur to prepare cathode slurries and the elimination of complex procedures to synthesize sulfur–carbon composites.

The electrochemical performances of the cathodes with or without a CNT film are summarized in figure 6(d). Compared to the Al/50S cathode, the Al/50S-CNT (100) cathodes showed an impressive capacity improvement of 20%, 30% and 43% at 0.2C, 0.5C and 1C, respectively. When the sulfur loading was increased to 60 wt%, this effect was even more significant, with a capacity improvement of 52% at 0.2C, 109% at 0.5C and 146% at 1C in the Al/60S-CNT (100) cathode. These results reveal that the CNT film can serve as an efficient built-in current collector and adsorption layer to bring out large capacities and reversibility, especially at high cycling rates and increased sulfur loadings. The capacities achieved here are comparable to those of sulfur cathodes recorded recently, such as the sulfur-hollow carbon sphere–graphene composite [30], sulfur-doped graphene [33], sulfur cathodes with a graphene oxide membrane [17], C/S nanocomposite [31], CNT/graphene–sulfur composite film [9], etc. Compared to some of the complex and energy-consuming synthesis methods used in other cathode structures, the cathode preparation from commercial pure sulfur and the very simple battery configuration in this work greatly lower the cost, simplify the fabrication procedure and provide promising potentials for large-scale production of Li-S batteries.

4. Conclusions

In conclusion, ultrathin and lightweight cross-stacked CNT film was employed as an additional built-in current collector and adsorption layer in sulfur cathodes, resulting in an impressive high-rate capability and excellent cycling performances. Compared to the conventional Al/S cathode, the Al/S-CNT cathode with high sulfur loading of 60 wt% exhibited a significantly enhanced electrochemical performance, with capacity improvement of 52%, 109% and 146% at 0.2C, 0.5C and 1C. The excellent battery performance of the Al/S-CNT cathode is ascribed to (1) the large conductivity of the cross-stacked CNT film that constructs embedded electron pathways for effective electron transfer; (2) the highly porous structure of the CNT film that provides abundant adsorption points to support sulfur cathode materials; and (3) the high flexibility and mechanical stability of the CNT film that adsorbs the strain and retains integrity in prolonged electrochemical processes. These appealing characteristics of the CNT film enable its potential application as a built-in layer to simplify the fabrication procedure and promote scaled-up production of Li-S batteries.

Acknowledgments

This work was supported by the National Basic Research Program of China (2012CB932301), the NSFC (51102146 and 51472141) and the Fundamental Research Funds for the Central Universities (2652015425).

References

[1] Ji X L and Nazar L F 2010 *J. Mater. Chem.* **20** 9821
[2] Manthiram A, Fu Y Z, Chung S H, Zu C X and Su Y S 2014 *Chem. Rev.* **114** 11751
[3] Manthiram A, Fu Y Z and Su Y S 2013 *Acc. Chem. Res.* **46** 1125
[4] Yin Y X, Xin S, Guo Y G and Wan L J 2013 *Angew. Chem. Int. Ed.* **52** 13186
[5] Xu G Y, Ding B, Pan J, Nie P, Shen L F and Zhang X G 2014 *J. Mater. Chem.* A **2** 12662
[6] Evers S and Nazar L F 2013 *Acc. Chem. Res.* **46** 1135
[7] Jin K K, Zhou X F, Zhang L Z, Xin X, Wan G H and Liu Z P 2013 *J. Phys. Chem.* C **117** 21112
[8] Guo J C, Xu Y H and Wang C S 2011 *Nano Lett.* **11** 4288
[9] Chen Y, Lu S T, Wu X H and Liu J 2015 *J. Phys. Chem.* C **119** 10288
[10] Wang H L, Yang Y, Liang Y Y, Robinson J T, Li Y G, Jackson A, Cui Y and Dai H J 2011 *Nano Lett.* **11** 2644
[11] Zhou G M, Pei S F, Li L, Wang D W, Wang S G, Huang K, Yin L C, Li F and Cheng H M 2014 *Adv. Mater.* **26** 625
[12] Ji X L, Lee K T and Nazar L F 2009 *Nat. Mater.* **8** 500
[13] Wang J L, Yang J, Xie J Y, Xu N X and Li Y 2002 *Electrochem. Commun.* **4** 499
[14] Su Y S and Manthiram A 2012 *Chem. Commun.* **48** 8817

[15] Su Y S and Manthiram A 2012 *Nat. Commun.* **3** 1166
[16] Wang X F, Wang Z X and Chen L Q 2013 *J. Power Sources* **242** 65
[17] Huang J Q, Zhuang T Z, Zhang Q, Peng H J, Chen C M and Wei F 2015 *ACS Nano* **9** 3002
[18] Han X G *et al* 2013 *Nano Energy* **2** 1197
[19] Jiang K L, Wang J P, Li Q Q, Liu L A, Liu C H and Fan S S 2011 *Adv. Mater.* **23** 1154
[20] Zhang X B, Jiang K L, Teng C, Liu P, Zhang L, Kong J, Zhang T H, Li Q Q and Fan S S 2006 *Adv. Mater.* **18** 1505
[21] Jiang K L, Li Q Q and Fan S S 2002 *Nature* **419** 801
[22] Liu K, Sun Y H, Liu P, Wang J P, Li Q Q, Fan S S and Jiang K L 2009 *Nanotechnology* **20** 335705
[23] Deng Z F, Zhang Z A, Lai Y Q, Liu J, Li J and Liu Y X 2013 *J. Electrochem. Soc.* **160** A553
[24] Chang B Y and Park S M 2010 *Annu. Rev. Anal. Chem.* **3** 207
[25] Hjelm A K and Lindbergh G 2002 *Electrochim. Acta* **47** 1747
[26] Lu S T, Cheng Y W, Wu X H and Liu J 2013 *Nano Lett.* **13** 2485
[27] Zhou G M, Yin L C, Wang D W, Li L, Pei S F, Gentle I R, Li F and Cheng H M 2013 *ACS Nano* **7** 5367
[28] Wang Z Y, Dong Y F, Li H J, Zhao Z B, Wu H B, Hao C, Liu S H, Qiu J S and Lou X W 2014 *Nat. Commun.* **5** 5002
[29] Zheng G Y, Yang Y, Cha J J, Hong S S and Cui Y 2011 *Nano Lett.* **11** 4462
[30] Zhou G M, Zhao Y B and Manthiram A 2015 *Adv. Energy Mater.* **5** 1402263
[31] Ma J, Fang Z, Yan Y, Yang Z, Gu L, Hu Y S, Li H, Wang Z and Huang X 2015 *Adv. Energy Mater.* **5** 6
[32] Wang J L, He Y S and Yang J 2015 *Adv. Mater.* **27** 569
[33] Ma Z L, Dou S, Shen A L, Tao L, Dai L M and Wang S Y 2015 *Angew. Chem.-Int. Ed.* **54** 1888